

Recovering volatility from option prices by evolutionary optimization

Sana Ben Hamida

Ecole Supérieure de Technologie et Informatique, Tunis, Tunisia

Rama Cont

Centre de Mathématiques Appliquées, CNRS–Ecole Polytechnique, F-91128 Palaiseau, France

We propose a probabilistic approach for estimating parameters of an option pricing model from a set of observed option prices. Our approach is based on a stochastic optimization algorithm which generates a random sample from the set of global minima of the in-sample pricing error and allows for the existence of multiple global minima. Starting from an independently and identically distributed population of candidate solutions drawn from a prior distribution of the set of model parameters, the population of parameters is updated through cycles of independent random moves followed by “selection” according to pricing performance. We examine conditions under which such an evolving population converges to a sample of calibrated models. The heterogeneity of the obtained sample can then be used to quantify the degree of ill-posedness of the inverse problem: it provides a natural example of a coherent measure of risk, which is compatible with observed prices of benchmark (“vanilla”) options and takes into account the model uncertainty resulting from incomplete identification of the model. We describe in detail the algorithm in the case of a diffusion model, where one aims at retrieving the unknown local volatility surface from a finite set of option prices, and illustrate its performance on simulated and empirical data sets of index options.

Introduction

Stochastic models of financial markets usually represent the evolution of the price of a financial asset as a stochastic process $(S_t)_{t \in [0, T]}$ defined on some probability space $(\Omega, \mathcal{F}, \mathbb{P})$. An option on S with maturity T then corresponds to a random variable H_T , whose value is revealed at T and depends on the behavior of the underlying asset S between 0 and T . For example, a call option with maturity T_i

This project has benefitted from a research grant by Europlace Institute of Finance. Part of this work was developed in the framework of a research project on model calibration at HSBC-CCF, Division of Market and Model Risk. Earlier versions were presented at Humboldt University (Berlin), the AMAM 2003 Congress, the Satellite meeting on Mathematical Finance (Nice), the IPM Workshop on Inverse Problems (Tehran), HSBC Quants seminar (June 2003), Université de Paris X (MODALX) CREST Financial Econometrics seminar, Institute for Mathematics and Applications, Minneapolis (April 2004) and Bernoulli Satellite Meeting on Monte Carlo and particle methods (Barcelona 2004). We thank Kasra Barkeshli, Pierre DelMoral, Randall Douc, Helyette Geman, Dominick Samperi and Franck Viollet for helpful discussions.

and strike price K_i is then a financial contract which pays out $\max(0, S_{T_i} - K_i) = (S_{T_i} - K_i)^+$ to the holder at the maturity date T_i . The main focus of option pricing theory has been to define a notion of value for such options and compute this value. In arbitrage-free markets, the assumption of linearity of prices leads to the existence of a probability measure \mathbb{Q} equivalent to \mathbb{P} such that the value $V_t(H)$ of a terminal pay-off H_T is given by

$$V_t(H_T) = B(t, T)E^{\mathbb{Q}}[H_T|\mathcal{F}_t] \quad (1)$$

where $B(t, T)$ is a discount factor. For option pricing purposes, it is sufficient to know this pricing measure \mathbb{Q} . For example, the value $C_t(T, K)$ of a call option with maturity T and strike K is given by

$$C_t(T, K) = B(t, T)E^{\mathbb{Q}}[(S_T - K)^+|\mathcal{F}_t] \quad (2)$$

Since the famous Black–Scholes model was introduced in 1973, option markets have evolved to become autonomous, organized markets with a fairly high degree of liquidity, especially for index options and foreign exchange options. In such markets, the market prices of a series of liquid options, which are often call or put options, are readily observed. These market prices are then used as a benchmark to “mark to market” or *calibrate* an option pricing model, which can then be used to compute prices of more complex (“exotic”) options or compute hedge ratios.

The well-known smile and skew patterns in market option prices have led to the development of option pricing models generalizing the Black–Scholes model: local volatility (diffusion) models, stochastic volatility models, models based on jump processes. The price to pay for more realistic models is the increased complexity of model calibration: as noted by Jacquier and Jarrow (2000), in the presence of complex models “the estimation method becomes as crucial as the model itself”.

The availability of market prices for options has also made it feasible to identify such pricing models from market prices of options: this can be done by parametrizing the pricing measure by some parameter $\theta \in E$ and choosing θ to match an observed set $(C_i^*(T_i, K_i), i = 1, \dots, I)$ of call option prices:

$$C_i^*(T_i, K_i; \theta) = B(t, T_i)E^{\mathbb{Q}^\theta}[(S_{T_i} - K_i)^+|\mathcal{F}_t], \quad i = 1, \dots, I \quad (3)$$

The parameter θ can be a finite-dimensional vector: this is the case, for instance, in the Heston stochastic volatility model (Heston 1993), the Merton jump-diffusion model or the CEV model. Alternatively, in the *non-parametric* approach, θ is identified with the local characteristics of the stochastic (risk-neutral) process S and is typically an element of an infinite-dimensional space: the local volatility function in the case of diffusion models (Dupire 1994) or the Lévy measure in the case of models with jumps (Cont and Tankov 2004).

Determining the model parameter θ to match the market prices of a set of benchmark options is known to practitioners as the “model calibration” problem:

01 it is the inverse problem associated to the option pricing problem. One of
 02 the difficulties in solving this inverse problem is that in practice the market
 03 information is insufficient to completely identify a pricing model: if the model
 04 is sufficiently rich, several sets of model parameters may be compatible with the
 05 market prices, leading to ill-posedness and model uncertainty.

06 Because of possible model mis-specification, it is neither feasible nor mean-
 07 ingful in practice to match exactly the market prices. Therefore, the calibration
 08 problem is often reformulated as an optimization problem, where the goal is to
 09 minimize the pricing error or discrepancy between model prices and market prices
 10 for a set of liquidly traded options. A common way to measure this discrepancy is
 11 to use the (quadratic) difference between market and model prices, which leads to
 12 the nonlinear least squares method:

13
 14
$$\inf_{\theta \in E} G(\theta), \quad G(\theta) = \sum_{i=1}^I |C^\theta(t, S_t, T_i, K_i) - C_t^*(T_i, K_i)|^2 w_i \quad (4)$$

 15
 16

17 where $w_i > 0$ is a weight, $C_t^*(T_i, K_i)$ is the market price of a call option observed
 18 at date t and C^θ is the model price computed with a parameter θ . However, the
 19 optimization problem (4) is not easy to solve. As a function of the parameter
 20 θ , the objective function G is neither convex nor does it have any particular
 21 structure enabling the use of gradient-based minimization methods to locate
 22 the minima. Also, $G(\cdot)$ is not given explicitly: its computation often involves
 23 a numerical method – either a finite difference solver, a Fourier transform or a
 24 Monte Carlo simulation – and computing its gradient may be even more difficult.
 25 More importantly, it is not clear whether G has a unique global minimum and,
 26 even if this is the case, whether the minimum can be reached by a gradient-based
 27 algorithm.

28 A remedy proposed in the literature (Avellaneda *et al* 1997; Coleman *et al*
 29 1999; Cont and Tankov 2004; Crépey 2003; Jackson *et al* 1999; Lagnado and
 30 Osher 1997) has been to use a *regularization* method, adding to the objective
 31 function (4) a convex penalization criterion $F : E \rightarrow \mathbb{R}^+$ which makes the prob-
 32 lem well-posed and for which a gradient-based optimization procedure can be
 33 used:

34
$$\inf_{\theta \in E} G(\theta) + \alpha F(\theta)$$

 35

36 Examples of penalization criteria are smoothness norms for volatility functions
 37 (Crépey 2003; Jackson *et al* 1999; Lagnado and Osher 1997) and relative entropy
 38 (Avellaneda *et al* 1997; Cont and Tankov 2004) for probability measures. When
 39 applied to a given set of market prices, these methods yield a single set of model
 40 parameters calibrated to the market but require the extra step of determining the
 41 regularization parameter α .

42 With or without regularization, deterministic optimization methods will at best
 43 locate one of the (local or global) minima of the fitting criterion, but have nothing
 44 to say about the multiplicity of solutions of the initial (non-regularized) calibration
 45

01 problem (4). In other words, they provide a point estimate but no information
02 about parameter uncertainty. However, the non-uniqueness of the solution of
03 the original calibration problem is not simply a mathematical nuisance: the
04 multiplicity of solutions contains interesting information on *model uncertainty*,
05 which is lost through the process of regularization.

06 We describe here a probabilistic approach to the model calibration problem,
07 which takes into account the multiplicity of solutions and reflects the ill-posed
08 character of the problem instead of suppressing it. Our method is based on a
09 stochastic algorithm, which generates a random sample from the set of calibrated
10 models. Starting from an independently and identically distributed (IID) popu-
11 lation of candidate solutions drawn from a prior distribution on the set of model
12 parameters, the population of parameters is updated through cycles of independent
13 random moves followed by “selection” using the calibration criterion. We examine
14 conditions under which such an evolving population converges to the set of global
15 minima of a pricing error such as (4), which may or may not be reduced to a single
16 element.

17 Our approach naturally leads to a *family* of pricing models compatible with
18 market prices. This family can then be used to quantify model uncertainty and its
19 impact on derivative prices and provides an example of a coherent risk measure
20 (Artzner *et al* 1999) compatible with a set of observed option prices.

21 While most of the existing literature on estimation of parameters from option
22 prices has approached the problem in the framework of a deterministic opti-
23 mization, yielding point estimates of model parameters (Andersen and Andreasen
24 2000; Avellaneda *et al* 1997; Coleman *et al* 1999; Crépey 2003; Cont and Tankov
25 2004; Jackson *et al* 1999), several authors (Ait Sahalia and Lo 1998; Jacquier and
26 Jarrow 2000; Lo 1986) have cast this problem into a statistical framework, which
27 leads to distributions on model parameters. Non-parametric kernel regression
28 was used in Ait Sahalia and Lo (1998) for estimation of state price densities
29 from option prices. This approach assumes IID errors across options and can
30 produce, in addition to state price density estimates, confidence intervals on such
31 estimates in large samples. In a contrast to these methods, we do not rely on
32 large sample results nor do we assume IID errors across options. Closer to the
33 spirit of this work, Jacquier and Jarrow (2000) propose a Bayesian approach in
34 the framework of the Black–Scholes model: starting from a prior distribution on
35 model parameters and an assumption on the distribution of observational errors,
36 a *posterior* distribution is obtained by taking into account the observed option
37 prices and a Monte Carlo algorithm is proposed for simulating from this posterior.
38 The general idea of our approach is similar: we start from a prior distribution on
39 model parameters, end up with a sample of model parameters and allow for model
40 mis-specification. However, our approach is based not on the application of the
41 Bayes formula but on the minimization of a pricing error such as (4) and does
42 not rely on a specific distribution for observational errors (which is not known in
43 practice). The computational complexity of the Bayesian approach has prevented
44 it from being applied beyond a simple case such as Black–Scholes. The scope of
45

01 application of our method is not limited to the Black–Scholes model, as illustrated
 02 by the example of diffusion models in Section 2.

03 Section 1 presents a general methodology for model identification based on a
 04 set of observed option prices, applicable to a wide range of models. Section 2
 05 specializes these results to the case of a one-dimensional diffusion model (“local
 06 volatility” model) and describes in detail the algorithm used in this case. In
 07 order to assess the performance of our method, we first perform some numerical
 08 experiments on simulated data; these tests are presented in Section 3. Section 4
 09 presents the results obtained by applying the method to an empirical data set of
 10 DAX option prices. Section 5 discusses the implications of our methodology for
 11 measuring model uncertainty and its extensions beyond the setting of diffusion
 12 models or European options.

13
 14 **1 Evolutionary algorithms for model calibration**

15 In this section we formulate a general framework for the model calibration
 16 problem and describe the use of a class of stochastic optimization methods, known
 17 as evolutionary algorithms, for solving it. After presenting the mathematical
 18 setting of the problem, we present the idea behind evolutionary optimization
 19 methods, their convergence properties and discuss how they apply in the context
 20 of model calibration.
 21

22
 23 **1.1 Model calibration as an optimization problem**

24 Consider an underlying asset modeled as stochastic process $(S_t)_{t \in [0, T]}$ on some
 25 probability space $(\Omega, \mathcal{F}, \mathcal{F}_t, \mathbb{P})$. Denote by $B(t, T)$ the discount factor, with
 26 $B(T, T) = 1$. An arbitrage-free pricing rule can be represented as a measure
 27 $\mathbb{Q} \sim \mathbb{P}$ such that the discounted price $\hat{S}_t = B(t, T)S_t$ is a martingale under \mathbb{Q} .
 28 Let $M(S)$ denote the set of such pricing rules. An option pricing model is given
 29 by a (parametrized) family of pricing measures:

30
 31
$$\theta \in E \rightarrow M(S) \tag{5}$$

32
 33
$$\theta \rightarrow \mathbb{Q}^\theta \tag{6}$$

34 For each $\theta \in E$, \mathbb{Q}^θ is a probability measure on E such that $(B(t, T)S_t)_{t \in [0, T]}$ is
 35 a martingale. Now consider a set of benchmark options, with terminal pay-offs
 36 denoted by $H_i, i = 1, \dots, I$. Typically these benchmark options are European
 37 calls and puts in the case of index or foreign exchange option markets, or caps and
 38 floors in the case of interest rate markets. However, for what follows we need not
 39 assume this is the case; the benchmark options may have path-dependent features,
 40 for example.

41 Denote by $C_i(\theta), i = 1, \dots, I$, the values of benchmark options at $t = 0$ under
 42 the pricing rule given by the parameter θ :

43
 44
$$C_i(\theta) = B(t, T)E^{\mathbb{Q}^\theta}[H_i | \mathcal{F}_0]$$

 45

We will assume the parameter-to-price map

$$C : E \mapsto \mathbb{R}^I$$

$$\theta \mapsto C(\theta) = (C_i(\theta), i = 1, \dots, I) \quad (7)$$

is continuous; this is the case for all option pricing models of interest. We now assume that the prices of these benchmark options are observed on the market at $t = 0$; denote these prices by C_i^* , $i = 1, \dots, I$. The pricing rule \mathbb{Q}^θ is said to be compatible with the market prices $(C_i^*)_{i=1, \dots, I}$ if

$$\forall i = 1, \dots, I, \quad C_i(\theta) = C_i^* \quad (8)$$

Equation (8) should be seen as a system of implicit constraints for the model parameter θ and the calibration problem consists of determining (the set of parameters) θ satisfying (8). However, (8) may have no solution at all. Typically, if the model is mis-specified, the observed option prices may not lie within the range of prices attainable by the model. Also, observed option prices are “noisy” estimates, defined up to a bid–ask spread: although they may be compatible, in the sense of bid–ask spreads, with the model prices for some parameter θ , they may not verify the equality (8) exactly for any given $\theta \in E$. For these reasons, it is a common approach to replace (8) by its least-squares version:

$$\inf_{\theta \in E} G(\theta), \quad G(\theta) = \sum_{i=1}^I w_i |C_i(\theta) - C_i^*|^2 \quad (9)$$

where $w_i > 0$ are a set of weights. In cases where the option prices $C_i(\theta)$ depend continuously on θ and when E is a compact subset of a finite-dimensional space (i.e. there is a finite number of bounded parameters), the least-squares formulation always admits a solution. However, the solution of (9) need not be unique: G may in fact have several *global* minima, when the observed option prices do not uniquely identify the model. Even in the case where there is a unique global minimum, it may be difficult to compute using gradient-based optimization methods commonly used for this purpose. As well as the fact that the gradient of G is often not known explicitly, in most cases G is a continuous but non-convex function: Figures 1–3 show examples of the function G for some popular parametric option pricing models, computed using a data set of DAX index options prices on 11 May 2001. Figure 1 corresponds to the quadratic pricing error in a log-normal–mixture diffusion model, described in Brigo and Mercurio (2002): it displays a flat profile, many parameter combinations yielding equivalent fits. The quadratic pricing error in the Heston stochastic volatility model (Heston 1993), shown in Figure 2 as a function of the “volatility of volatility” and the mean-reversion rate, displays a line of local minima. Finally, the pricing error for the Variance Gamma model (Madan and Milne 1991) in Figure 3 displays a strongly non-convex profile, with two distinct minima in the range of observed values.

01
02
03
04
05
06
07
08
09
10
11
12
13
14
15
16
17
18
19
20
21
22
23
24
25
26
27
28
29
30
31
32
33
34
35
36
37
38
39
40
41
42
43
44
45

FIGURE 1 Error surface for the log-normal density mixture model, DAX options.

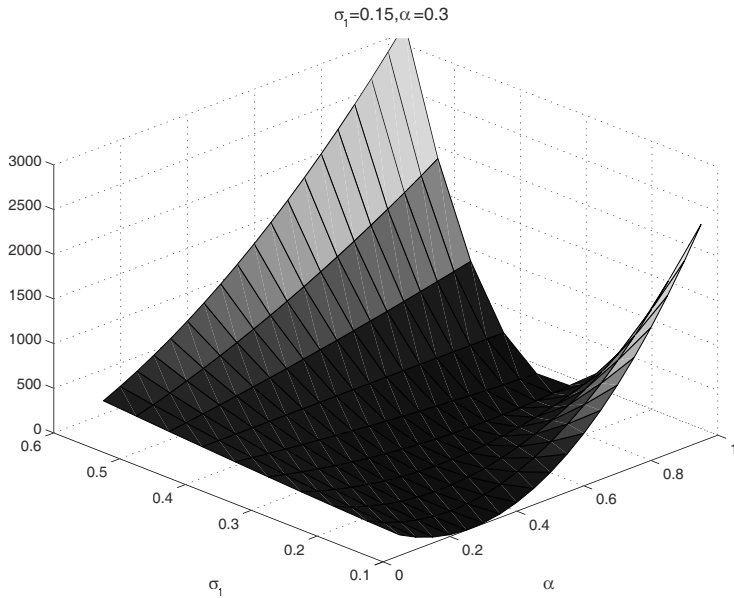


FIGURE 2 Error surface for the Heston stochastic volatility model, DAX options.

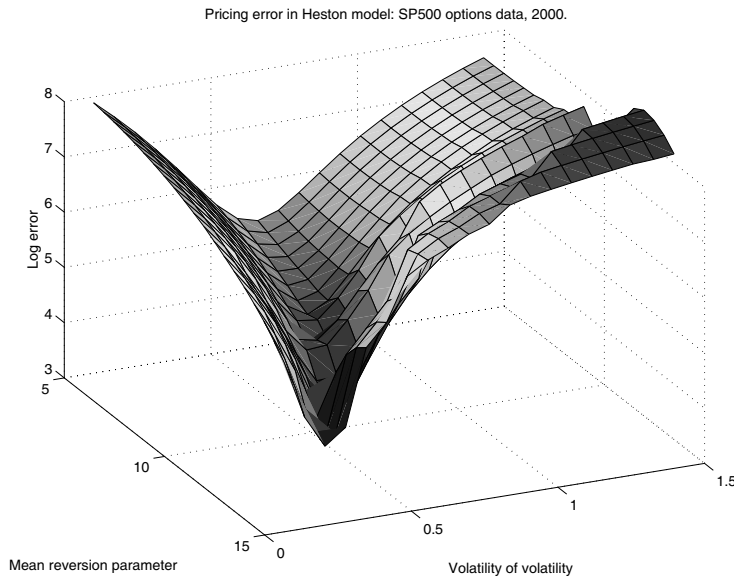
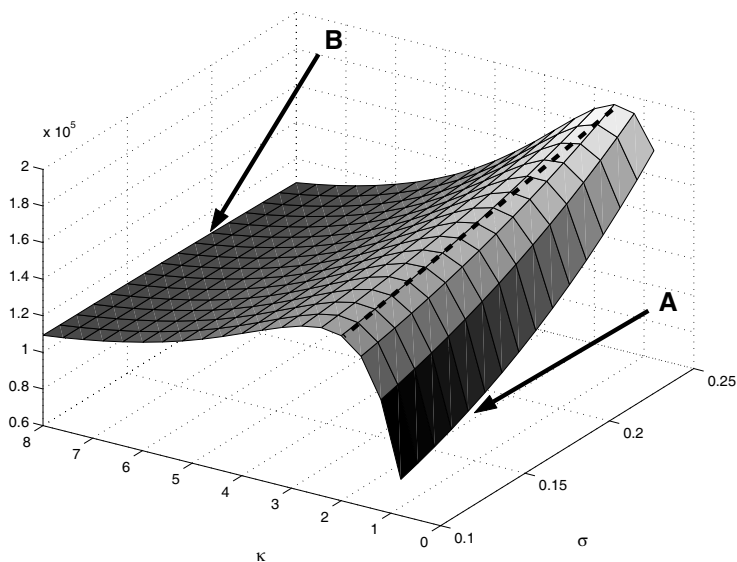


FIGURE 3 Error surface for the Variance Gamma (pure jump) model, DAX options.



From Figures 1–3 it is readily observed that, given the prices of the benchmark call and put options, there are several – sometimes a full range of – model parameters which are equally compatible with these market prices. In any of these (real) examples, gradient-based algorithms will converge to local minima of G or, at best, to *one* of the global minima of G , leaving us uninformed about the other possible solutions and their multiplicity. The existence of multiple solutions is not due to a specific numerical optimization method, but inherent to the ill-posedness of the problem at hand: instead of ignoring or bypassing it using an exogenous criterion, it is thus interesting to explore the various solutions and try to quantify the associated model uncertainty. We will now describe a probabilistic approach, based on *evolutionary optimization*, which attempts to *sample* from the set of solutions of (9), instead of selecting one of them using an exogenous criterion.

1.2 Evolutionary optimization: a brief overview

Evolutionary algorithms, introduced in Holland (1975), are order-zero stochastic optimization methods: they require neither differentiability nor convexity of the functions being optimized. Evolutionary algorithms are based on a random search of the parameter space by a population of optimizers undergoing “evolutionary pressure” based on an analogy with Darwinian selection of species (Holland 1975; Bäck 1995). They are widely used to solve complex – high-dimensional and nonconvex – optimization problems (Kallel *et al* 2001). This section gives an overview of evolutionary algorithms and their convergence properties.

01 Consider a search space E and a continuous ‘fitness’ function $G : E \mapsto [0, \infty[$
 02 to be minimized on E . In practice E will be taken to be a compact set but
 03 this condition is not strictly necessary. An evolutionary algorithm with objective
 04 function G is based on the evolution of a population of candidate solutions
 05 (*individuals*), denoted by $X_n^N = (\theta_n^i, i = 1, \dots, N)$, where n is the current step
 06 (*generation*), N is the population size and θ_n^i is a candidate minimizer of G . For
 07 $X = (\theta^1, \dots, \theta^N) \in E^N$ denote $[X] = \{\theta^1, \dots, \theta^N\}$.

08 The idea is to “evolve” the population $\theta_n^i, i = 1, \dots, N$, through cycles of
 09 modification (mutation) and selection in order to improve the performance of
 10 its individuals, as measured by the fitness function G . At each iteration n , the
 11 population undergoes three transformations:

$$12 \quad X_n^N \xrightarrow[\text{mutation}]{} V_n^N \xrightarrow[\text{crossover}]{} W_n^N \xrightarrow[\text{selection}]{} X_{n+1}^N \quad (10)$$

13
 14
 15 During the mutation stage, individuals undergo independent random transforma-
 16 tions, as if performing independent random walks in E , resulting in a randomly
 17 modified population V_n^N . In the crossover stage, pairs of individuals are chosen
 18 from the population to “reproduce”: each pair gives birth to a new individual,
 19 which is then added to the population. This results in a new diversified population
 20 W_n^N , regrouping parents and children, with $> N$ elements. This new population
 21 is now evaluated using the fitness function $G(\cdot)$: we compute $G(x)$ for every $x \in$
 22 $[W_n^N]$. Elements of the population are now selected for survival according to their
 23 fitness: those with a lower value of G have a higher probability of being selected.
 24 One such selection rule is the following: each individual $x \in [W_n^N]$ is selected with
 25 probability proportional to $\exp[-\beta_n G(x)]$. Here $\beta_n > 0$ is a parameter called the
 26 selection pressure: $\beta_n \rightarrow \infty$ leads to elitist selection, retaining only the individuals
 27 with lowest values of $G(\cdot)$ while $\beta_n \rightarrow 0$ means we select individuals at random,
 28 regardless of their performance. The N individuals thus selected then form the
 29 new population, X_{n+1}^N .

30 The role of mutation is to explore the parameter space and the optimization is
 31 done through selection. The idea is that, by analogy with Darwinian evolution,
 32 cycles of mutation followed by selection will globally improve the population’s
 33 performance and lead it to regions where $G(\cdot)$ is minimal. Note that the gradient of
 34 G is not used at any time: movements are totally random, corrected only through
 35 the selection procedure. Crossover is used to enhance the search in parameter
 36 space. Aside from the crossover step, the mutation–selection cycle is similar to
 37 the prediction–correction step in the EM algorithm or in filtering problems. The
 38 flow chart in Algorithm 1 summarizes the structure of an evolutionary algorithm.

39 In mathematical terms, Algorithm 1 corresponds to simulating an (inhomo-
 40 geneous) Markov chain $(X_n^N)_{n \in \mathbb{N}}$ in E^N (Nix and Vose 1991):

- 41 • The initial population is an IID sample drawn from a prior distribution μ_0
 42 on E :

$$43 \quad \theta_0^i \stackrel{\text{IID}}{\sim} \mu_0, \quad i = 1, \dots, N$$

01 **ALGORITHM 1**02
03 $n \leftarrow 0$ 04
05 Draw N IID points in E from prior distribution $\mu_0: \theta_0^i \sim \mu_0$.
06 Initialize population $X_0^N = (\theta_0^1, \theta_0^2, \dots, \theta_0^N)$ 07
08 Evaluate X_0^N : compute $G(\theta_0^i)$, $i = 1, \dots, N$ 09
10 **while** (desired fitness level not reached)**do**11
12 **begin**13 $n - 1 \rightarrow n$ 14 Mutation: randomly modify individuals in $X_{n-1}^N \mapsto V_n^N$ 15 Generate new individuals by crossover $\mapsto W_n^N$ 16 Evaluate W_n^N : compute $G(x)$, $x \in [W_n^N]$ 17 Select X_n^N from W_n^N 18
19 **end**

- 20
-
- 21
-
- 22 •
- Mutation*
- . Each individual
- θ^i
- evolves independently following a transition
-
- 23 kernel
- $M_n(x, dy)$
- on
- E
- .
-
- 24 •
- Selection*
- . At the
- n
- th iteration, given the population
- θ_n^i
- ,
- $i = 1, \dots, N$
- , each
-
- 25 individual
- θ_n^i
- is selected with probability
- $\exp[-\beta_n G(\theta_n^i)]$
- ; if not selected, it
-
- 26 is replaced by another individual
- θ_n^j
- selected with probability

27
28
$$\frac{\exp[-\beta_n G(\theta_n^j)]}{\sum_{k=1}^N \exp[-\beta_n G(\theta_n^k)]}$$

29
30 The selection pressure β_n is progressively increased: $\beta_n \rightarrow \infty$ as $n \rightarrow \infty$.

- 31 •
- Crossover*
- . Each pair
- (θ^i, θ^j)
- is selected according the selection mechanism
-
- 32 above and then evolves following a transition kernel
- C_n
- on
- E^2
- .

33
34 Asymptotics and concentration properties of mutation–selection algorithms have
35 been studied (Cerf 1996; Cerf 1998; Del Moral and Miclo 2000; Del Moral
36 and Miclo 2001; Del Moral and Miclo 2003; Löwe 1996) using “small noise”
37 asymptotics and large deviation techniques. Most studies are limited to mutation–
38 selection algorithms, not including crossover, which complicates the picture. In
39 what follows, we will give convergence results in the framework where there is
40 no crossover. These results give various conditions on the mutation and selection
41 kernel under which, for large n the population becomes concentrated on the set of
42 minima of G .43 A first set of results (Cerf 1996; Cerf 1998) states that, when E is finite and for
44 a large enough population size $N \geq N_0$, if the mutation allows us to sufficiently

01 explore the parameter space and the mutation noise is gradually decreased to zero
 02 as $n \rightarrow \infty$ then the population gradually settles down on the set of global optima
 03 of G .

04 The approach we adopt here is to study the distribution of individuals in large
 05 populations ($N \rightarrow \infty$) (Del Moral and Miclo 2000; Del Moral and Miclo 2001).
 06 In this framework one considers the primary object to be, not the positions (θ_n^i) of
 07 the individuals, but the population distribution $\mu_n^N = N^{-1} \sum_{i=1}^N \delta_{\theta_n^i}$, which then
 08 defines a flow $(\mu_n^N)_{n \geq 0}$ on $M_1(E)$, the space of probability measures on E . Under
 09 some technical conditions on the mutation and selection kernels (Del Moral 2004),
 10 the flow μ_n^N weakly converges as $N \rightarrow \infty$ to a distributional flow $(\mu_n)_{n \geq 0}$ given
 11 by the measure-valued dynamical system¹

$$13 \quad \mu_{n+1} = \mu_n M_n S_{\mu_n}^n \quad (11)$$

14 where mutation and selection steps are represented by (nonlinear) transformations
 15 acting on μ_n : M_n is the mutation kernel at the n th generation and S_{μ}^n is a (state-
 16 dependent) transition kernel corresponding to the selection rule

$$19 \quad S_{\mu}^n(x, dy) = e^{-\beta_n G(x)} \delta_x(dy) + (1 - e^{-\beta_n G(x)}) \frac{e^{-\beta_n G(y)} \mu(dy)}{\int \mu(dz) \exp[-\beta_n G(z)]} \quad (12)$$

21 Conditions under which this convergence is uniform with respect to $n \geq 0$ are
 22 given in Del Moral *et al* (2001): the distribution of the individuals in the
 23 evolutionary algorithm X_n^N then behaves like a sample from μ_n as $n \rightarrow \infty$.
 24 The Markov chain $(X_n^N)_{n \geq 0}$ described above then corresponds to a N -particle
 25 approximation of the measure-valued dynamical system (11). The goal is then to
 26 choose the mutation kernels M_n and the selection parameter β_n such that when
 27 $n \rightarrow \infty$ the distribution μ_n concentrates on the minima of G . By contrast with the
 28 situation described in Cerf (1998), finiteness of E is not needed. Also, one can
 29 keep the mutations time-homogeneous and concentrate the population on the set
 30 of optima by gradually increasing the selection rate β_n as $n \rightarrow \infty$ (Del Moral and
 31 Miclo 2003).

32 Denote by $H(Q|P)$ the relative entropy of a probability distribution Q with
 33 respect to P and define

$$35 \quad I(\mu) = \inf_K \int_E \mu(dx) H(K(x, \cdot) | M(x, \cdot)) \quad (13)$$

37 where the infimum is taken over all Markov kernels with stationary measure μ .
 38 The following result (Del Moral and Miclo 2003, Proposition 4.2.) shows that
 39 if the mutation kernel verifies a mixing condition and the selection pressure is
 40 progressively increased, the population concentrates in the level set corresponding
 41 to the “minimum” of G in the following sense.

43
 44 ¹Here, μM designates the action of M on the measure μ : $\mu M(dy) = \int_E \mu(dx) M(x, dy)$.

01 PROPOSITION 1 (Asymptotic behavior when $n \rightarrow \infty$) Let G be a function of
 02 bounded oscillation, choose $\beta_n = n^a$, $a \in]0, 1[$, and assume the mutation kernel
 03 $M_n = M$ satisfies the following mixing condition:

$$04 \quad \exists \epsilon > 0, \text{ such that } \forall (x, y) \in E^2, M(x, \cdot) \geq \epsilon M(y, \cdot) \quad (14)$$

06 Then the population concentrates in the level set corresponding to G^* :

$$08 \quad \forall \delta > 0, \quad \mu_n(G(\theta) \geq G^* + \delta) \rightarrow 0 \text{ as } n \rightarrow \infty$$

10 where G^* is the solution of the variational problem

$$12 \quad G^* = \inf \left\{ \int_E G(\theta) \mu(d\theta), \mu \in M_1(E), I(\mu) < \infty \right\} \quad (15)$$

14 We will see in Section 2 that, under appropriate conditions on the kernel M , G^*
 15 coincides with the essential infimum of G with respect to the invariant measure of
 16 the kernel M .

17 Another interesting property of this Markov chain, usually known under the
 18 (obscure) name of “propagation of chaos”, states the following: under some
 19 technical conditions and if the initial population is IID, when population size
 20 $N \rightarrow \infty$, the joint law of any finite subset $(\theta_n^1, \dots, \theta_n^k)$ (k fixed) of individuals
 21 converges weakly to a product law.² This result can be interpreted as follows:
 22 when the population size N is large, the individuals in each finite subpopulation
 23 $(\theta_n^1, \dots, \theta_n^k)$ will behave as if they were independent. This suggests the following
 24 statistical interpretation. If N is large, then for large n a finite subpopulation
 25 $(\theta_n^1, \dots, \theta_n^k)$ can be viewed as a sample of *independent* draws from the level
 26 set $\{x \in E, G(x) \leq G^* + \delta\}$: one can use the evolutionary algorithm to obtain a
 27 sample of independent δ -optima from the function G .

29 1.3 Evolutionary algorithms for model calibration

31 Now consider the setting of option pricing models described in Section 1.1. We
 32 consider the pricing error $G : E \mapsto [0, \infty[$ defined by

$$34 \quad G(\theta) = \sum_{i=1}^I w_i |C_i(\theta) - C_i^*| \quad (16)$$

36 where $C_i(\theta)$ are model prices and C_i^* are observed (transaction or mid-market)
 37 prices for the benchmark options. We will assume that the parameter space E
 38 is compact: in most cases, it is simply a compact subset of \mathbb{R}^d . If the model
 39 is capable of perfectly fitting the data, then $\min G = 0$ otherwise $\min G > 0$.
 40 However, even if $\min G = 0$ we are not necessarily interested in computing the
 41

43 ²We refer to Del Moral and Miclo (2000) for a precise formulation of results on propagation of
 44 chaos for evolutionary algorithms and other particle systems.

01 zeros of G . Recall that mid-market or transaction prices C_i^* are defined up to a
 02 bid–ask interval $[C_i^{\text{bid}}, C_i^{\text{ask}}]$. Thus, it is not meaningful for a model to retrieve the
 03 value of C_i^* with a precision much higher than $|C_i^{\text{bid}} - C_i^{\text{ask}}|$. Now define the *a*
 04 *priori* error level δ by

$$05 \quad \delta = \sum_{i=1}^I w_i |C_i^{\text{bid}} - C_i^{\text{ask}}| \quad (17)$$

06
 07 Given the uncertainty on option values due to bid–ask spreads, one cannot mean-
 08 ingfully distinguish a “perfect” fit $G(\theta) = 0$ from any other fit with $G(\theta) \leq \delta$.
 09 Therefore, all parameter values in the level set $\{\theta \in E, G(\theta) \leq \delta\}$ correspond to
 10 models which are compatible with the market data $(C_i^{\text{bid}}, C_i^{\text{ask}})_{i=1, \dots, I}$. As noted
 11 before, in general the evolutionary algorithm described above allows the level
 12 $G^* \geq \min G$ given by (15) to be reached. We will later see that under some
 13 conditions G^* coincides with the (essential) infimum of G . If $G^* > \delta$ then *no*
 14 *model* in the class considered is capable of reproducing market prices with the
 15 required accuracy and the model is clearly mis-specified. Thus, we will assume in
 16 what follows that

$$17 \quad G^* \leq \delta \quad (18)$$

18
 19 We will see that this assumption can indeed be verified in all empirical examples
 20 given below. In this case the level set $\{\theta \in E, G(\theta) \leq \delta\}$ is not empty: some
 21 parameter values will satisfy the calibration requirement within the desired
 22 accuracy, and our objective will be to sample from this set.

23 When (18) is satisfied, under the conditions of Proposition 1, the evolutionary
 24 algorithm yields a population of points which converges to a sample of model
 25 parameters compatible with the market data $(C_i^{\text{bid}}, C_i^{\text{ask}})_{i=1, \dots, I}$ in the sense that
 26 $G(\theta) \leq \delta$. Note that this means that, as $n \rightarrow \infty$, elements of the population end
 27 up in the level set $\{\theta \in E, G(\theta) \leq \delta\}$ so we obtain not only one solution but a
 28 *population* of model parameters calibrated to market data. Using the “propagation
 29 of chaos” property described above, one can sample a subpopulation of such
 30 parameters and regard it as a sample of statistically independent draws from the
 31 set of calibrated model parameters.

32 Compared to existing algorithms for estimating model parameters from option
 33 prices, evolutionary optimization methods present the following advantages.

- 34 • No interpolation of option prices is required. Contrary to implied tree (Der-
 35 man *et al* 1996) methods or methods based on the Dupire formula (Dupire
 36 1994), we does not require call–put prices for all strikes or maturities nor
 37 any ad hoc interpolation of observed prices. They can therefore be applied
 38 to index options where the number of observations is large ($I \simeq 100\text{--}200$)
 39 but also to equity options for which data is scarcer ($I \simeq 20\text{--}30$).
- 40 • They avoid computing the (high-dimensional) gradient of the objective
 41 function, an essential but difficult step in other algorithms.
- 42 • They do not require convexity of the objective function to be minimized. As
 43 seen in Figures 1 and 2, this property does not hold in many commonly used
 44 models.

- Evolutionary algorithms provide a *population* of solutions instead of a single one: model uncertainty is reflected in the heterogeneity of this population.

We will now present a case study to show how this methodology can be used to estimate parameters of an option pricing model from market data.

2 Recovering diffusion coefficients from option prices

The methodology outlined above is quite general and is not tied to a certain class of option pricing models. However, to illustrate its performance in a specific example, we will now specialize it to the class of Markovian diffusion models, popular in option pricing applications, where the underlying asset is modeled as a diffusion process:

$$\frac{dS_t}{S_t} = \mu(t, S_t) dt + \sigma(t, S_t) dW_t \quad (19)$$

The model parameter here is the *local volatility function* $\sigma(\cdot, \cdot)$. The calibration problem then consists of identifying the local volatility function $\sigma(S, t)$ from prices of call or put options observed in the market. This is usually done by parametrizing the volatility function with some parameter $\theta \mapsto \sigma_\theta$ and minimizing the quadratic pricing error over parameter values $\theta \in E$:

$$G_2(\theta) = \sum_{i=1}^I w_i |C^{\sigma_\theta}(t, S_t, T_i, K_i) - C_t^*(T_i, K_i)|^2 \quad (20)$$

here $C_t^*(T_i, K_i)$ is the market price of a call option with strike K and maturity T and $C^\sigma(\cdot, \cdot, T_i, K_i)$ is the model price. The model price is obtained as the solution of the partial differential equation (PDE)

$$\begin{cases} \forall S > 0, t \in [0, T[, & \frac{\partial C^\sigma}{\partial t} + \frac{\sigma^2(t, S)S^2}{2} \frac{\partial^2 C^\sigma}{\partial S^2} - rS \frac{\partial C^\sigma}{\partial S} = rC(t, S; T, K) \\ C^\sigma(T, S, T, K) = (S - K)^+ \end{cases} \quad (21)$$

Various numerical methods have been proposed for estimating local volatility functions from call option prices. Dupire (1994) presents a formula for reconstructing local volatility functions from a continuum of call option prices; however, this formula involves taking derivatives from discrete data and is numerically unstable. A discretized version of the Dupire formula is the implied tree method of Derman *et al* (1996), which is prone to similar instabilities leading to “negative probabilities”. Other methods, based on nonlinear least squares (Coleman *et al* 1999) or regularized versions of it (Achdou and Pironneau 2002; Avellaneda *et al* 1997; Crépey 2003; Jackson *et al* 1999; Lagnado and Osher 1997; Samperi 2002) all lead to minimization problems which are solved using gradient-based algorithms.³ In the non-parametric case, the minimization variable is the function

³See Crépey (2003) for a review.

01 $\sigma(\cdot, \cdot)$. After discretization, this leads to a (non-convex) minimization problem in
 02 a high-dimensional space, which presents the following difficulties.

- 03 • The gradient of G is costly to compute. This makes gradient-based opti-
 04 mization methods rather time consuming.
- 05 • The objective function G is not convex and typically presents many (local
 06 or global) minima. As a consequence, gradient-based methods tend to get
 07 trapped in local minima. Also, lack of convexity creates problems when
 08 using duality techniques as in Avellaneda *et al* (1997) and Samperi (2002),
 09 and may lead to a duality gap.

10 We will now describe how the evolutionary algorithm described above can be
 11 adapted to the reconstruction of local volatility functions from option prices and
 12 how it allows us to overcome these problems.

14 **2.1 An algorithm for reconstructing local volatility**

15 Evolutionary optimization algorithms are often criticized for their slow conver-
 16 gence; however, much of this criticism is due to the use of black-box evolution
 17 operators embedded in general-purpose libraries, which may have no relation
 18 with the problem at hand. In our case, *a priori* knowledge of the structure of
 19 local volatility functions will allow us to design the Markov chain in a way that
 20 improves considerably the convergence and accuracy of the algorithm.

21 The ingredients of the algorithm are the following.

- 23 1. A pricing algorithm (in this case, a finite-difference solver) which takes as
 24 input a local volatility function, a strike and a maturity and returns the value
 25 of the option in the model (19): $[\sigma(\cdot, \cdot), K, T] \rightarrow C^\sigma(T, K)$.
- 26 2. A parametrization of the set of admissible local volatility surfaces:

$$\begin{aligned}
 27 \quad & E \mapsto H \\
 28 \quad & \theta \mapsto \sigma_\theta(\cdot, \cdot) \tag{22}
 \end{aligned}$$

30 where H is a space of smooth functions $[0, T] \times \mathbb{R} \rightarrow \mathbb{R}^+$ which satisfy
 31 our *a priori* assumptions on the behavior of a local volatility function.

- 32 3. A prior distribution μ_0 on E summarizing our prior information on the local
 33 volatility function $\sigma(\cdot, \cdot)$: its level, its degree of smoothness, etc.
- 34 4. A set of market prices of call options: $C^* = (C^*(T_i, K_i), i = 1, \dots, I)$.
- 35 5. An objective function to be minimized on E : while (20) is a common
 36 choice, it should be noted that the only reason for using squared errors is
 37 to obtain differentiability. Since the evolutionary algorithm does not require
 38 differentiability of the objective function, instead of the quadratic pricing
 39 error we can also use the absolute pricing error which yields more stable
 40 numerical values:

$$41 \quad G(\theta) = \sum_{i=1}^I w_i |C^{\sigma_\theta}(t, S_t, T_i, K_i) - C_i^*(T_i, K_i)| \tag{23}$$

44 We now describe each of these ingredients in more detail.

2.2 Representation of the local volatility surface

We consider a representation similar to the one adopted in Jackson *et al* (1999). Consider a tenor $\mathbb{T} = \{T_1, \dots, T_L\}$ of maturities and let $\Delta x > 0$ be a positive number representing the resolution of the representation in the log-strike–price dimension and $x_k = k\Delta x$, $k = -K, \dots, 0, \dots, K$. For each maturity $T \in \mathbb{T}$ we represent the local volatility function $\sigma(T, \cdot)$ as a function of log-price $x = \ln(S/S_0)$ in the following way.⁴ For any maturity $T \in \mathbb{T}$, we represent $\sigma(T, \cdot)$ as a cubic spline:

$$\forall i = 1, \dots, L, \quad \sigma_\theta(T_i, \cdot) = \sum_{m=0}^M \theta(i, m) \phi_m(\cdot) \quad (24)$$

where $\phi_0(S) = 1$ is the constant function equal to 1 and $(\phi_m, m = 1, \dots, M)$ is the B-spline basis associated with the “knots” $(x_k, k = -K, \dots, 0, \dots, K)$, described in Appendix A. For $t \notin \mathbb{T}$, we define $\sigma(t, x)$ by linear interpolation: if $t \in [T_i, T_{i+1}]$ we set

$$\sigma(t, x) = \frac{T_{i+1} - t}{T_{i+1} - T_i} \sigma(T_i, x) + \frac{t - T_i}{T_{i+1} - T_i} \sigma(T_{i+1}, x) \quad (25)$$

For $t > T_n$ or $t < T_1$ we extrapolate by

$$\forall t > T_n, \quad \sigma(t, x) = \sigma(T_n, x) \quad (26)$$

$$\forall t < T_1, \quad \sigma(t, x) = \sigma(T_1, x) \quad (27)$$

In practice, all coefficients $\theta(i, m)$ are taken to be bounded: they are positive and bounded from above by some positive number, say c . Denote by H the space of local volatility functions generated in this way. H is a subset of a finite-dimensional space of smooth functions $[0, T] \times \mathbb{R} \mapsto \mathbb{R}$. A smooth local volatility surface $\sigma(\cdot, \cdot) \in H$ is thus represented by the matrix of nd coefficients, which we will denote by $\theta = [\theta(i, m), m = 0, \dots, M, i = 1, \dots, L] \in [0, c]^d$. $\sigma(\cdot, \cdot)$ will be positive if these coefficients are positive. This representation separates the “Black–Scholes” component, represented by the coefficients $\theta(\cdot, 0)$ from the other coefficients $\theta(i, m), m = 1, \dots, M$ which represent the implied volatility smile or skew.

2.3 Generating the initial population

The first step in the evolutionary algorithm is to generate a family of local volatility functions $\sigma_0^j(\cdot, \cdot), j = 1, \dots, N$, which constitute the initial population of candidate solutions. As described in Section 1, we generate this initial population using some prior distribution on the local volatility surface, capturing the information available on its level and shape.

⁴By abuse of notation, we continue to denote by $\sigma(t, x)$ the volatility in the log-price variable.

01 What prior information do we possess on local volatility functions? First, the at-
 02 the-money implied volatilities can give a good idea of the level of local volatilities:
 03 by analogy with a Black–Scholes model with time-varying volatility, we can set
 04 the constant (level) component $\theta(\cdot, 0)$ according to

$$05 \quad \forall T_i \in \mathbb{T}, \quad \theta(i, 0) = \sqrt{\frac{T_{i+1} \Sigma_{\text{ATM}}^2(T_{i+1}) - T_i \Sigma_{\text{ATM}}^2(T_i)}{T_{i+1} - T_i}} \quad (28)$$

06 where $\Sigma_{\text{ATM}}(T)$ is the at-the-money implied volatility for the maturity T . Apart
 07 from this, the only other prior requirement we might have is to require the local
 08 volatility to be “smooth” in (t, x) : in practice, this means that we want to avoid
 09 highly oscillatory behavior. To integrate this requirement we use a *smoothness*
 10 *prior*, i.e. a prior distribution on H which generates surfaces which are typically
 11 smooth as a function of price (and to a lesser extent, in the time variable). In order
 12 to quantify the smoothness we can use, for instance, the (semi)-norm

$$13 \quad \|\sigma\|_{1,2}^2 = \sum_{T \in \mathbb{T}} \int_0^T dt \int_{-A}^A dx \left[\left| \frac{\partial^2 \sigma}{\partial x^2}(t, x) \right|^2 + \left| \frac{\partial \sigma}{\partial t}(t, x) \right|^2 \right] \quad (29)$$

14 A possible choice of smoothness prior is then to choose a Gaussian measure
 15 restricted to E with density:

$$16 \quad \frac{a}{(2\pi)^{LM/2}} \exp \left[-\frac{\|\sigma\|_{1,2}^2}{2\gamma^2} \right] \quad (30)$$

17 where a is a normalization constant. A typical draw from this Gaussian measure
 18 will thus be a surface σ with $\|\sigma\|_{1,2}$ of the order γ ; hence the parameter γ can be
 19 used to control the smoothness of surfaces generated from this prior.

20 To simulate from this prior we use the representation (24). Each surface $\sigma(\cdot, \cdot)$
 21 is represented by its coefficients $\theta = [\theta(i, m), i = 1, \dots, n, m = 0, \dots, M] \in$
 22 \mathbb{R}^d and the smoothness semi-norm (29) can be written as a quadratic form in θ ,
 23 given by Equation (A.7) in Appendix A and can thus be written as

$$24 \quad \|\sigma\|_{1,2}^2 = {}^t \theta A \theta \quad (31)$$

25 where A is a $d \times d$ matrix. We set the reference level $\theta(i, 0)$ using the at-the-
 26 money implied volatility according to (28), and use a Cholesky decomposition to
 27 find a matrix B such that $A = BB^t$. We then set

$$28 \quad \theta^i(\cdot, \cdot) = B \cdot \epsilon^i, \quad i = 1, \dots, N \quad (32)$$

29 where $(\epsilon^i, i = 1, \dots, N)$ are IID $N(0, I_d)$ vectors.⁵ Note that smoothness norms
 30 such as (29) have also been used in Crépey (2003) and Jackson *et al* (1999) as
 31 regularization terms in order to penalize $G(\cdot)$. Using a smoothness prior as defined
 32 here allows us to introduce information on the smoothness of the volatility surface
 33 via the prior, *without* modifying the objective function G .

34 ⁵Note that, in fact, since the coefficients $\theta(i, m)$ are bounded the actual distribution corresponds
 35 to a truncated Gaussian distribution, values larger than the bounds being rejected and replaced
 36 by new ones.

2.4 Computation of the objective function

We choose as weights in the objective function

$$w_i = \max\left(\frac{1}{\text{vega}(T_i, K_i)}, 100\right)$$

where $\text{vega}(T_i, K_i)$ is the Black–Scholes vega of the option computed using the market implied volatility. This weight “converts” errors in price into errors in implied volatility, thus rescaling all terms in the sum defining G to the same order of magnitude. Thresholding by 100 avoids overweighting of options very far from the money. In order to compute the objective function at each step, the option prices $C^\sigma(t_0, S_0; T_i, K_i)$ have to be computed from the volatility surface $\sigma(\cdot, \cdot)$ and substituted in (23). This can be done in principle by solving the PDE (21) to compute $C^\sigma(t, S; T, K)$. The price we are interested in is then given by $C^\sigma(t_0, S_0; T, K)$. This method implies solving (21) at each time step for *each* option in the observation set. In the case where the calibration instruments are European call options, this procedure can be speeded up by a factor equal to the number of options being calibrated, by remarking that the call option price $C(t_0, S_0, T, K)$, as a function of the strike and maturity (K, T) , verifies the Dupire equation (Dupire 1994):

$$\begin{aligned} \frac{\partial C}{\partial T} + Kr \frac{\partial C}{\partial K} - \frac{K^2 \sigma^2(T, K)}{2} \frac{\partial^2 C}{\partial K^2} &= 0 \\ \forall K \geq 0, \quad C(t_0, S, t_0, K) &= (S - K)^+ \end{aligned} \quad (33)$$

Solving this equation will then give us the whole range of call prices for all strikes and maturities in a single sweep. Using a logarithmic change of variable $x = \ln(K/S_0)$ and $u(T, x) = C(t_0, S_0; T, S_0 e^x)$, (33) is equivalent to

$$\begin{aligned} \frac{\partial u}{\partial T} &= \frac{\sigma^2}{2} \frac{\partial^2 u}{\partial x^2} - \left(\frac{\sigma^2}{2} + r(t)\right) \frac{\partial u}{\partial x} \\ \forall x \in]-\infty, \infty[, \quad u(0, x) &= (S_0 - S_0 e^x)^+ \end{aligned} \quad (34)$$

Equation (34) is then localized to a bounded domain $x \in [-A, A]$ and discretized using an implicit finite difference scheme on a uniform grid. Unconditional stability of the implicit scheme reduces the number of time steps and allows us to use coarser grids in the first stages of the evolution and refine progressively as the need for precision appears. For the localized problem we use the numerical boundary conditions

$$u(T, A) = 0, \quad u(T, -A) = S_0(1 - e^{-A}) \quad (35)$$

which correspond to the asymptotic behavior of call prices for small and large strikes. The instantaneous discount rate $r(t)$ is modeled as a piecewise constant function computed from a set of discount factors with maturities $\{T_1, \dots, T_L\}$.

01 **2.5 The evolution scheme**

02 As described in Section 1, the population of parameters undergoes a cycle of
 03 mutation, crossover and selection at each iteration. In the case of volatility
 04 functions, we need to ensure that these transformations allow us to sufficiently
 05 explore the parameter space but avoids generating pathological volatility functions
 06 with non-smooth or oscillating features.

- 07
- 08 • *Mutation.* The mutation step amounts to randomly modifying each volatility
 09 function by adding a noise term to the spline coefficients. Noise terms
 10 are IID across individuals in the population but in order to conserve the
 11 smoothness of the surfaces, they cannot be IID across spline components.
 12 We choose them to have the covariance A defined in (A.7):

13
$$\forall j \in \{1, \dots, N\}, \forall i = 1, \dots, n, \quad \theta^j(i, \cdot) \leftarrow \theta^j(i, \cdot) + B \cdot \epsilon^j$$

14 where $\epsilon^j \sim N(0, I_M)$ are IID across individuals and B is as described in
 15 Section 2.3. More precisely, since E is bounded, moves beyond the imposed
 16 bounds are rejected: denoting the modified population by $V_n^N = (\gamma_n^i, i =$
 17 $1, \dots, N)$ we have

18
$$\gamma_n^j(i, \cdot) = \begin{cases} \theta_n^j(i, \cdot) + B \cdot \epsilon^j & \text{if } \theta_n^j(i, \cdot) + B \cdot \epsilon^j \in [0, c]^d \\ \theta_n^j(i, \cdot) & \text{if } \theta_n^j(i, \cdot) + B \cdot \epsilon^j \notin [0, c]^d \end{cases}$$

19 The mutation kernel M is thus a “truncated” Gaussian kernel:

20
$$M(x, dy) = M(x, x)\delta_x(dy) + 1_{y \in E} \frac{\exp[-\frac{1}{2}(y-x)A^{-1}(y-x)]}{\sqrt{(2\pi)^d|A|}} dy$$

21 where

22
$$M(x, x) = 1 - N(x, A)([0, c]^d) \tag{36}$$

23 is the probability that the mutation leaves the point x unmodified and
 24 $N(x, A)$ is the normal distribution centered at x with covariance A .

- 25 • *Selection.* At the n th iteration, given the population $\theta_n^i, i = 1, \dots, N$, each
 26 individual σ_n^i is selected with probability $\exp[-\beta_n G(\theta_n^i)]$; if not selected, it
 27 is replaced by another individual θ_n^j selected according to the distribution

28
$$\frac{\exp[-\beta_n G(\theta_n^j)]}{\sum_{k=1}^N \exp[-\beta_n G(\theta_n^k)]}$$

29 The selection parameter is increased with the number of iterations:

30
$$\beta_n = n^a \quad \text{with } 0 < a < 1$$

- 31
- 32 • *Crossover.* This extra step is not strictly required for convergence but
 33 enhances the search procedure in practice. First, we select, using the
 34 selection procedure outlined above, two individuals σ^j and σ^k from the

population. The probability of an individual being selected is therefore proportional to its calibration performance. Then, we generate an independent uniform random variable $\alpha \in [0, 1]$ and create a new individual σ^l by convex combination: $\sigma^r = \alpha\sigma^j + (1 - \alpha)\sigma^k$. σ^r is then added to the current population. Note that this operation preserves smoothness of the surfaces since

$$\|\sigma^r\|_{1,2} \leq \alpha\|\sigma^k\|_{1,2} + (1 - \alpha)\|\sigma^j\|_{1,2}$$

Neglecting the effect of the crossover step in the convergence analysis, we obtain the following convergence result, a proof of which is outlined in Appendix B.

PROPOSITION 2 (Convergence to global minima) *Let μ_n denote the distribution of the population after n mutation–selection cycles described above. Then, as $n \rightarrow \infty$, μ_n concentrates on the set of global minima of the pricing error G :*

$$\forall \epsilon > 0, \quad \mu_n \left(G(\theta) \geq \min_E G + \epsilon \right) \xrightarrow{n \rightarrow \infty} 0.$$

3 Numerical experiments

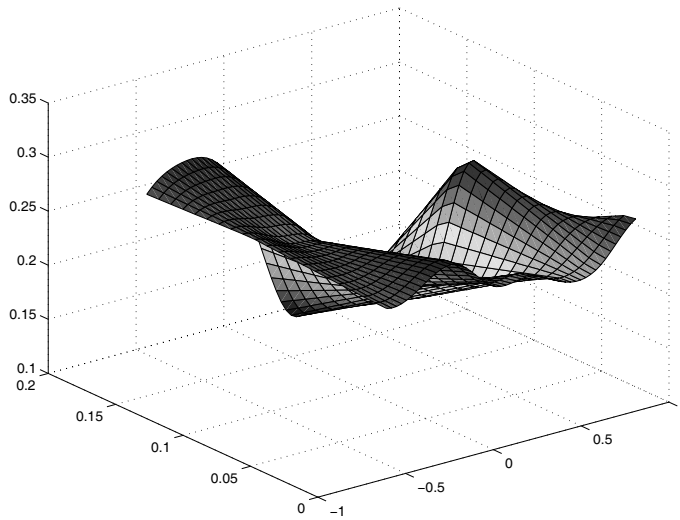
To assess the performance of the algorithm we perform a series of numerical tests in which the algorithm is used to retrieve a known diffusion coefficient (i.e. local volatility function) from a set of option prices generated from it.

Figure 4 shows the local volatility function $\sigma_0(\cdot, \cdot)$ used for the test.⁶ A set of call option prices $C^*(0, S_0, T_i, K_i)$ was computed from $\sigma_0(\cdot, \cdot)$ by solving the Dupire PDE (33). In order for the test set to be similar to the empirical data sets available to us, we used 70 unevenly spaced values of strikes and maturities for (T_i, K_i) , $i = 1, \dots, 70$. To each of these prices, we add independent noise components with standard deviation equal to 0.1% of the option price; this observational noise simulates the effect of bid–ask spreads in real data.

These prices are then used as inputs for the calibration algorithm described in Section 2. A population of $N = 50$ solutions was used in this case. Volatility functions were parametrized as described in Section 2.2, using a tenor of 3 maturities and 10 spline nodes per maturity. Figure 5 illustrates the evolution of the population: the performance (measure with G) of the average individual, the best individual as well as the standard deviation of the population performance converge after 15 iterations to values very close to zero, which indicates a population of local volatility functions with very good calibration performance. The *a priori* error defined in (17) is normalized here to $\delta = 1$: we therefore see that in this case $G^* \ll \delta$ and the level set $\{\theta \in E, G(x) \leq \delta\}$ is attained. These local volatility functions, although very similar with regard to calibration performance, can be quite different in their actual values: Figure 6 shows some of the best

⁶This function was actually obtained by calibrating a diffusion model to DAX option prices, as described in Section 4.

FIGURE 4 Local volatility function $\sigma_0(\cdot, \cdot)$ used to generate option prices in the numerical experiments.



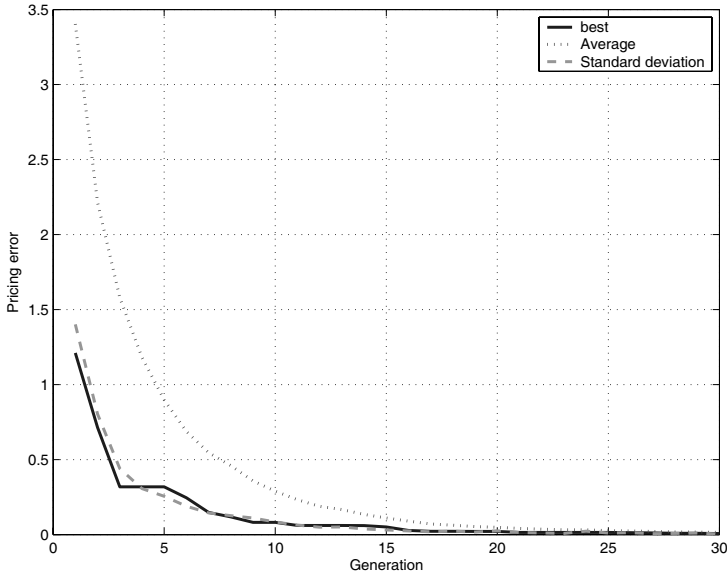
performing ones. Figure 7 shows the retrieval error in terms of implied volatility. Each point represents the calibration error in implied volatility units for one option in the data set. As shown in the figure, the input implied volatilities are retrieved with a precision of a few basis points, which is quite acceptable by comparison to market bid–ask spreads.

To summarize, these numerical tests show that the evolutionary algorithm is capable of retrieving a local volatility function from a data set of option prices with realistic size and features. Not only does the algorithm retrieve the input local volatility function and its associated implied volatilities with a precision of a few basis points, it also identifies *other* local volatility functions which are different but which lead to similar prices for the benchmark options in the calibration set: they correspond to volatility functions which are not distinguishable from σ_0 given only the observed option prices.

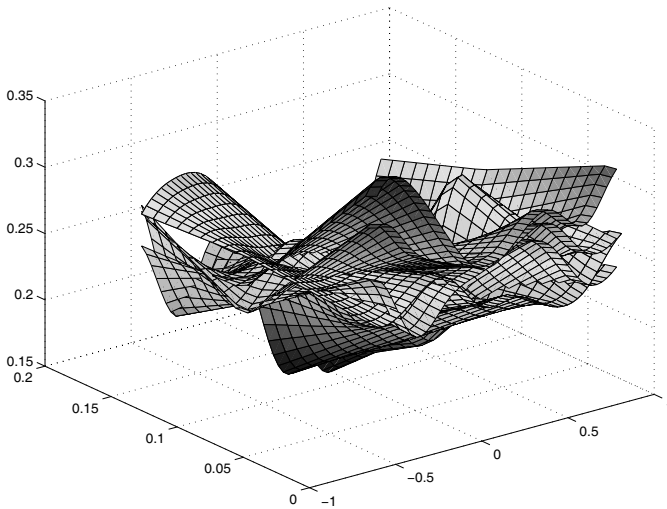
4 Empirical results: DAX index options

Motivated by the positive results in the numerical experiments, the algorithm described above was applied to a data set of market prices of European call and put options on the DAX index, quoted on 13 June 2001. Around 100 option prices were available to us on this date, with different strikes and maturities running from a week up to one year. Figure 8 shows the implied volatility of these options as a function of strike and maturity. Options with a Black–Scholes vega less than 0.01 were discarded from the calibration set: such options are too far from the money

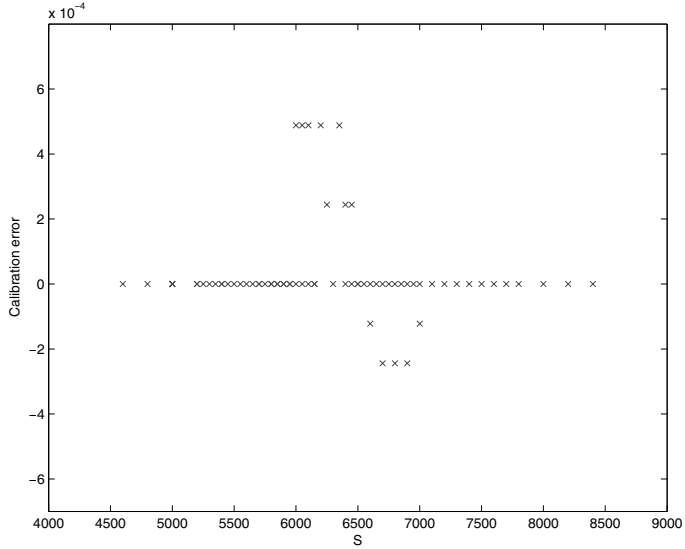
01 **FIGURE 5** Numerical test: population mean, standard deviation of fitness and fitness
02 of best individual.
03



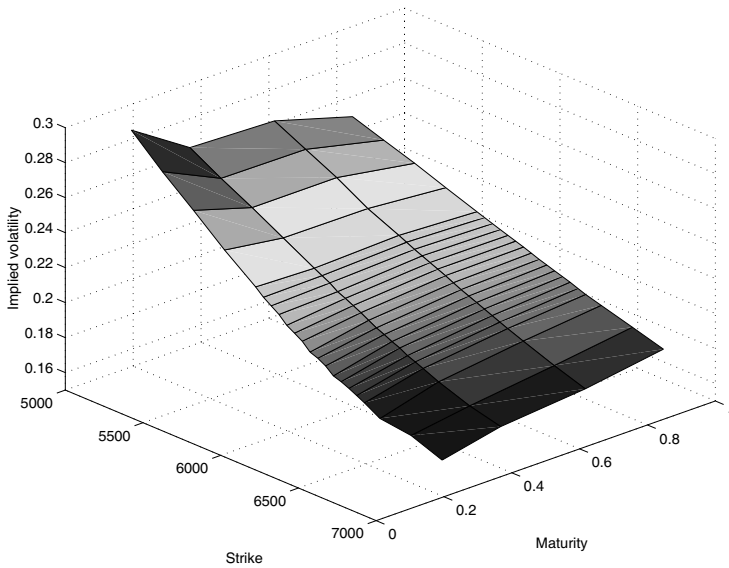
22
23
24 **FIGURE 6** Local volatility functions retrieved from option prices generated by $\sigma_0(\cdot, \cdot)$.
25



01 **FIGURE 7** Numerical test: retrieval error in terms of implied volatility. Each point
 02 represents the calibration error in implied volatility units for one option in the data
 03 set. Scale: $10^{-4} = 1$ basis point.
 04



22
 23
 24 **FIGURE 8** DAX options implied volatilities: 13 June 2001.
 25



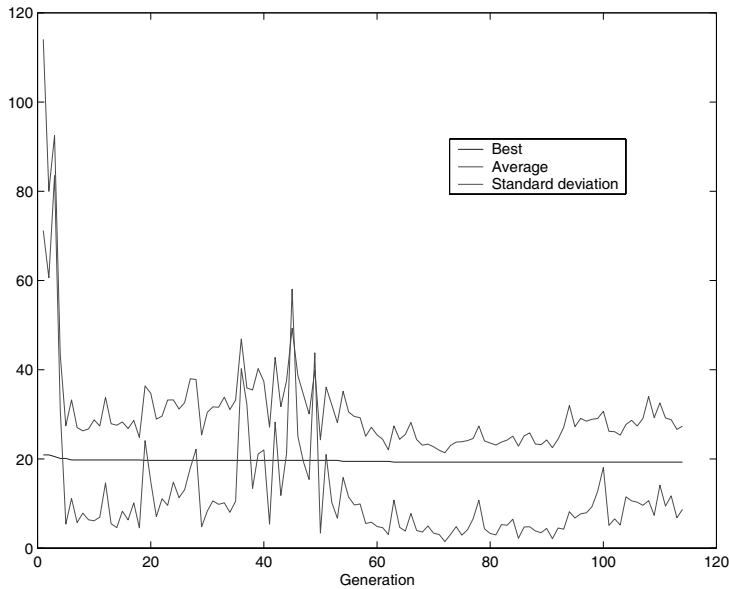
01 to be liquid and the uncertainty on implied volatility is too large to be useful in
02 our context. The weight w_i was chosen as described in Section 2.4. In this way,
03 the i th error term in (23) is, up to first order in the pricing error, equivalent to the
04 error in implied volatility units.

05 The procedure described in Section 2 was applied to this data set to generate a
06 population of 50 candidate solutions, which were then evolved using an evolution-
07 ary algorithm. Figure 9 illustrates the convergence of the algorithm: contrary to
08 the numerical tests shown above where the model was known to be well specified,
09 here convergence is not monotonous, indicating that the minimization is more
10 difficult. The *a priori* error defined in (17) is given in this case by $\delta \simeq 40$: again,
11 we observe that the level set $\{\theta \in E, G(x) \leq \delta\}$ has been attained. Note that fitness
12 in the population is fairly homogeneous as indicated by a standard deviation
13 of $G(\theta^i)$ much lower than its population average. This means that most of the
14 models in the population have a similar (and good) calibration performance. It
15 is therefore interesting to see if they correspond to similar volatility functions.
16 Figure 10 shows two of the best performing volatility functions obtained. As
17 seen in the figure, they have different term structures, distinguishable by the eye.
18 However, their calibration performance, as indicated by the absolute pricing error
19 (23), is quite similar. Figure 11 gives the decomposition of the pricing errors for
20 these two local volatility models: each point on the graphs corresponds to the
21 calibration error, in implied volatility units, for one of the options in the data set.
22 Since there is a one-to-one map between local volatility functions and call option
23 prices (Dupire 1994), if *all* strikes and maturities had been included in the data
24 sets we would have been able to distinguish these two models; however, as can be
25 observed from Figure 11, the two diffusion models display quite similar patterns
26 of implied volatility for the quoted strikes and maturities. Other local volatility
27 functions, compatible with the same data set of call options, are given in Figure 12:
28 they can be regarded as a sample drawn from the set of calibrated local volatility
29 functions. Recall that the final population has a relatively small standard deviation
30 of fitness so the calibration performance of the corresponding diffusion models
31 are quite similar, even though the actual values of local volatilities and their term
32 structures differ. What is striking is the inhomogeneity in (t, S) of their dispersion,
33 which decreases notably as a function of maturity. For the sake of clarity we
34 have represented the pointwise upper and lower envelopes of these surfaces in
35 Figure 13: the widening of this band as maturity decreases reflects the parabolic
36 nature of the inverse problem. In financial terms, it simply means that short-term
37 options are not affected much by the value of the underlying (local) volatility
38 so their price cannot give much information on short-term volatility, leading to
39 a large uncertainty on short-term volatility. Conversely, longer-term options are
40 strongly affected by the value of volatility so one can use them to obtain more
41 precise estimates for longer term volatility.

42 Similar results were obtained with DAX options on other dates. These exam-
43 ples illustrate that the possibility of being able to reconstruct local volatility
44 from call option prices in a precise manner is at best illusory: even in the case

45

01 **FIGURE 9** Evolution of pricing error.
 02



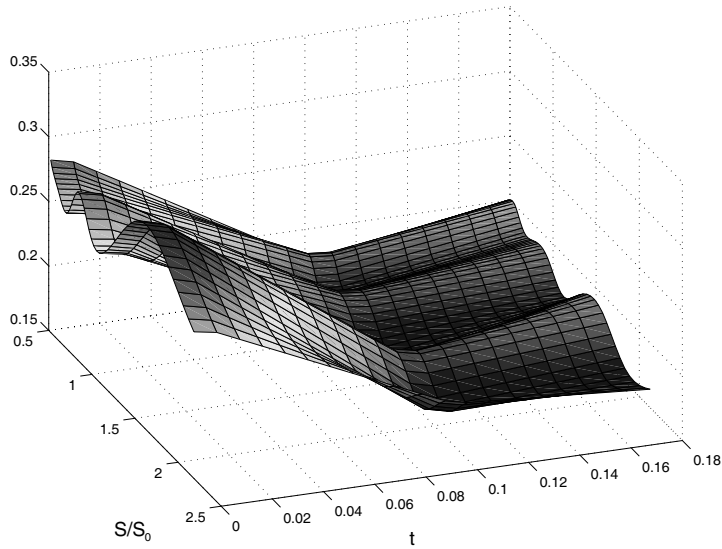
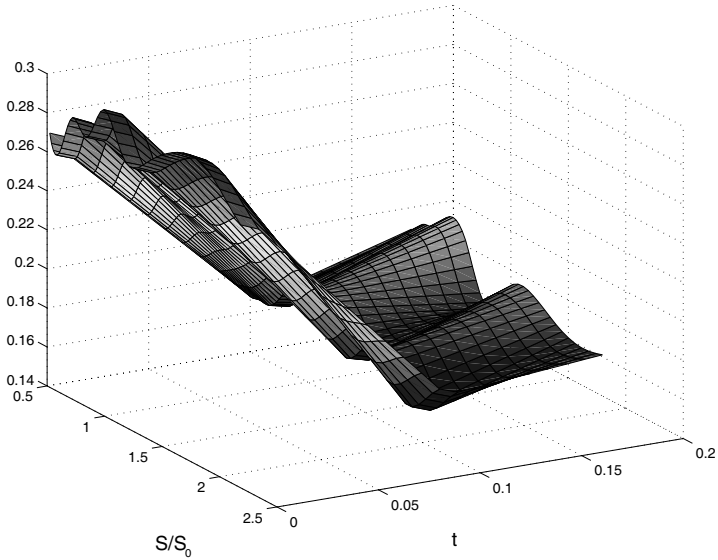
23 of index options where data sets are relatively large, the parameter uncertainty
 24 which prevails is too important to be ignored. They also show that this uncertainty
 25 prevails even more for short maturities: in our example, short-term volatility
 26 hovers anywhere between 15% and 35%! These observations cast a doubt on the
 27 information content of short-term options in terms of volatility and question the
 28 basis of short-maturity asymptotics as a method for exploring volatility patterns.
 29

30 **5 Applications and extensions**
 31

32 We have described a new approach for the estimation of the (risk-neutral)
 33 dynamics of an underlying asset from cross-sectional observations of option
 34 prices. Our approach is based on an evolutionary algorithm in which a population
 35 of optimizers performs a random search in the parameter space of the model,
 36 evolving through cycles of random mutation followed by selection. We give
 37 conditions under which the algorithm converges to a sample of models calibrated
 38 to the market prices with a given precision.

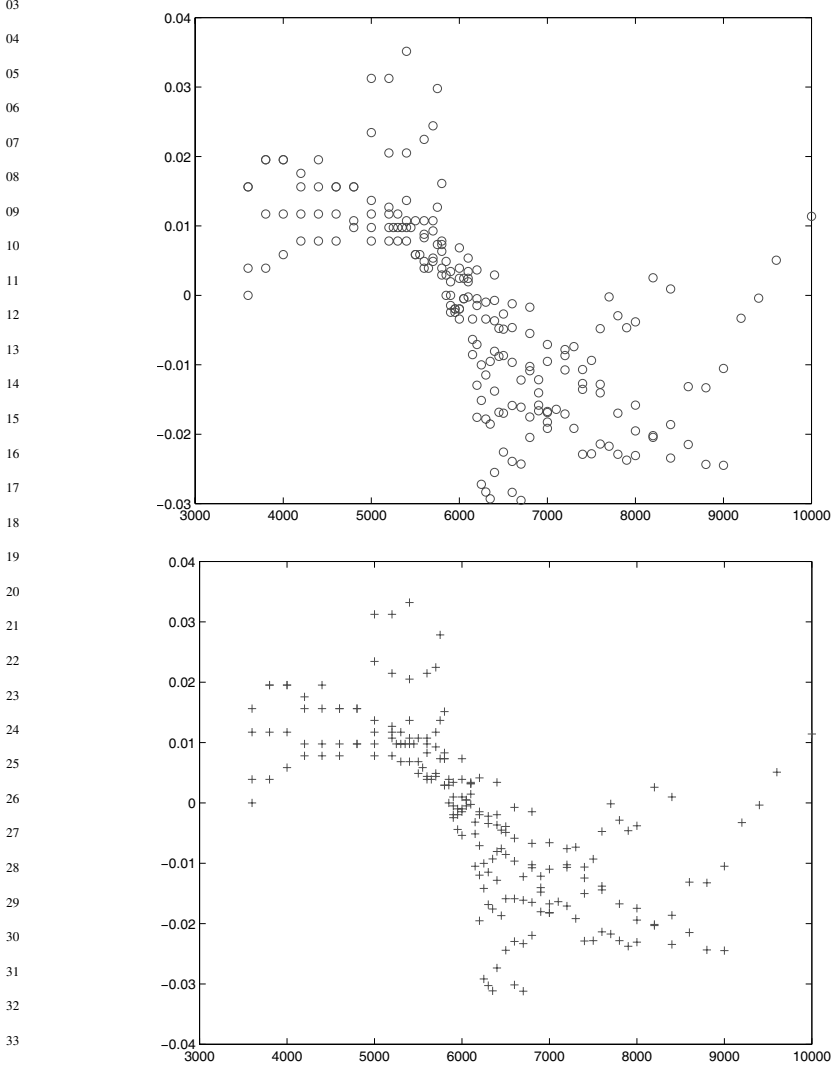
39 The proposed algorithm takes market prices for a set of benchmark options
 40 as the input and produces a family of models which are marked-to-market on
 41 these options. We have given a detailed example of how this algorithm can be
 42 implemented in the case of diffusion models, where the aim is to reconstruct
 43 the local volatility surface from prices of call options and we have illustrated its
 44 implementability by applying it to an empirical data set of index options.
 45

01 **FIGURE 10** Local volatility surfaces: DAX options.
 02



40 Evolutionary algorithms require neither differentiability nor convexity of the
 41 objective function to be minimized and hence allow a wide range of fitting
 42 criteria to be used. They avoid computation of gradients, which are the main
 43 computational burden in high-dimensional optimization problems typical of non-
 44 parametric calibration methods. In fact, their only requirement is being able to
 45

01 **FIGURE 11** Calibration error in implied volatility units: DAX options.
 02



35
36
37 price the options in the calibration set which makes them easy to adapt to a wide
38 variety of models and pay-offs.

39
40 **5.1 Quantifying model uncertainty**
41

42 Apart from the numerical advantages detailed above, it also yields, as a by-
43 product, a way to analyze model uncertainty. Calibration algorithms based on
44 deterministic optimization yield a *point estimate* for model parameters: they point
45

FIGURE 12 A sample of local volatility surfaces calibrated to DAX options.

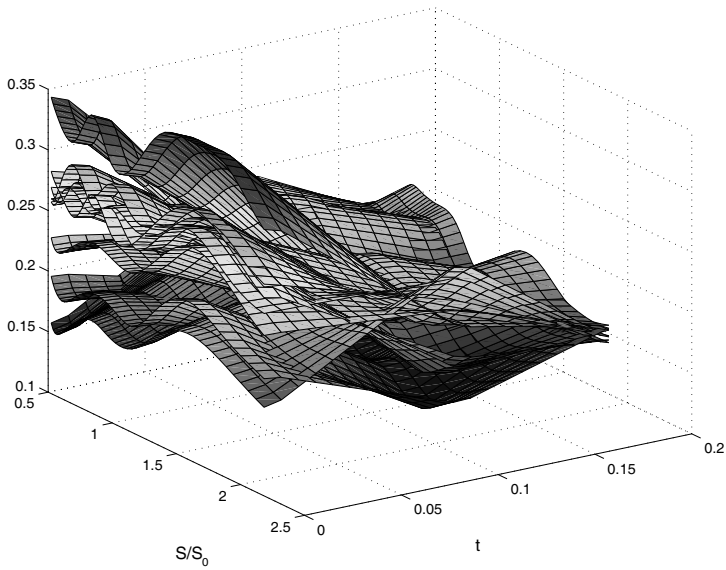
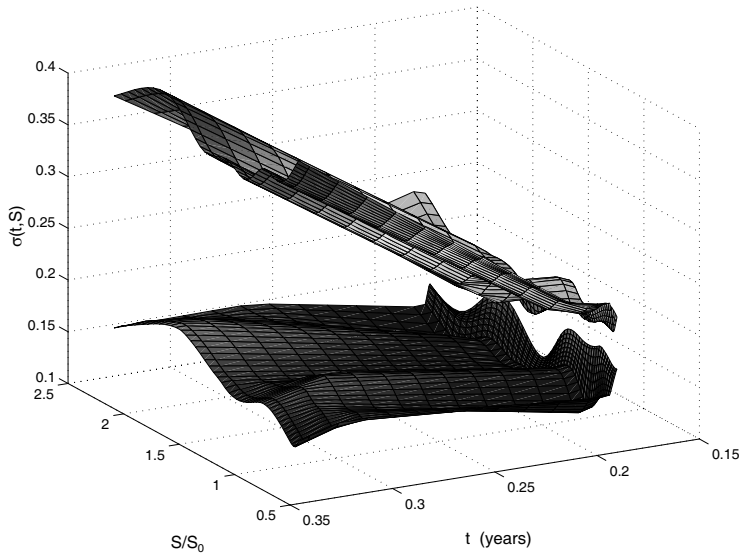


FIGURE 13 Pointwise confidence intervals for the local volatility $\sigma(t, S)$ computed from ten best solutions. $\sigma_{\min}(t, S)$ and $\sigma_{\max}(t, S)$: DAX options.



to *one* model in the class of models considered (here, the Markovian diffusion class) which approximates the observed prices of benchmark options well. By contrast, an evolutionary approach yields an entire *population* of solutions to the inverse problem, many of which price the benchmark options with equivalent precision. The heterogeneity of this population reflects the uncertainty in model parameters, which are left undetermined by the benchmark options. This idea can be exploited to produce a quantitative measure of model uncertainty compatible with observed market prices of benchmark instruments Cont (2006), in the following manner. Suppose that we have calibrated a model $(\mathbb{Q}_\theta)_{\theta \in E}$ to the benchmark pay-offs H_i with market prices C_i^* , $i = 1, \dots, I$, using the evolutionary algorithm outlined above. This yields a set of parameters $\theta_1, \dots, \theta_k$ corresponding to calibrated models. Denote the associated pricing rules by $\mathcal{Q} = \{\mathbb{Q}_{\theta_1}, \dots, \mathbb{Q}_{\theta_k}\}$. Then for $\mathbb{Q} \in \mathcal{Q}$ we have $E^{\mathbb{Q}}(H_i) \simeq C_i^*$ within bid–ask bounds. Now consider an exotic or illiquid option on the same underlying asset, with pay-off X . Define the upper and lower price bounds by

$$\bar{\pi}(X) = \sup_{\mathbb{Q} \in \mathcal{Q}} E^{\mathbb{Q}}[X], \quad \underline{\pi}(X) = \inf_{\mathbb{Q} \in \mathcal{Q}} E^{\mathbb{Q}}[X] = -\bar{\pi}(-X) \quad (37)$$

Then $\bar{\pi}(X)$ is a coherent risk measure (Artzner *et al* 1999), compatible with the market prices in the sense that for any of the traded options with pay-offs H_i , $i = 1, \dots, I$, $\bar{\pi}(H_i) \simeq C_i^*$ within bid–ask bounds. This is in contrast with super-replication costs associated with uncertainty in volatility, which are typically way out of market bid–ask bounds. Furthermore

$$\mu(X) = \bar{\pi}(X) - \underline{\pi}(X) \quad (38)$$

quantifies the impact of model uncertainty on the value of the derivative X . Once the family \mathcal{Q} is obtained from the evolutionary calibration procedure, computation of $\bar{\pi}(X)$, $\underline{\pi}(X)$ and $\mu(X)$ simply amounts to pricing the claim X in each of the models; moreover, the model realizing the supremum can be identified as the “worst case” model for the claim X . Therefore, our model calibration procedure enables us to quantify the uncertainty on values of contingent claims associated with parameter uncertainty, without much further computational effort. Properties of such measures of model uncertainty are further discussed in Cont (2006).

5.2 Extensions

As noted above, since the only ingredient necessary in the calibration algorithm is the computation of option prices, one can also include prices of options other than European calls or puts in this setting: American options, barrier options or any other available exotic options can also be included in the calibration set as long as an efficient numerical algorithm is available for pricing them in the model. To our knowledge, this is not feasible using alternative calibration algorithms.

On the implementation side, the methodology described in Section 1 is not specific to diffusion models: the same approach can be used for other families

of models such as stochastic volatility models, interest rate models, multivariate models and models with jumps. We believe these extensions are of interest for applications and will be the object of our future work.

Appendix A B-splines

Define the functions

$$\psi_0(x) = \frac{1}{6}(1 - x)^3 \tag{A.1}$$

$$\psi_1(x) = \frac{1}{6}(4 - 6x^2 + 3x^3) \tag{A.2}$$

$$\psi_2(x) = \frac{1}{6}(1 + 3x + 3x^2 - 3x^3) \tag{A.3}$$

$$\psi_3(x) = \frac{x^3}{6} \tag{A.4}$$

Given a set of nodes $X_0 < X_1 < \dots < X_n$ the functions $(\psi_i, i = 0, \dots, 3)$ may be translated and dilated appropriately by substituting for x the new variable

$$\xi_{[X_{i-1}, X_i]} = \frac{x - X_{i-1}}{X_i - X_{i-1}} \tag{A.5}$$

The *B-spline* basis $(\phi_i, i = 0, \dots, n)$ associated with a set of nodes $X_0 < X_1 < \dots < X_n$ is defined by

$$\phi_i(x) = \begin{cases} 0 & x \leq X_{i-2} \\ \psi_3(\xi_{[X_{i-2}, X_{i-1}]}(x)) & X_{i-1} \geq x \geq X_{i-2} \\ \psi_2(\xi_{[X_{i-1}, X_i]}(x)) & X_i \geq x \geq X_{i-1} \\ \psi_1(\xi_{[X_i, X_{i+1}]}(x)) & X_{i+1} \geq x \geq X_i \\ \psi_0(\xi_{[X_{i+1}, X_{i+2}]}(x)) & X_{i+2} \geq x \geq X_{i+1} \\ 0 & x \geq X_{i+2} \end{cases}$$

Smooth functions may then be built by using linear combinations of B-splines:

$$f(x) = \sum_{i=1}^n f_i \phi_i(x) \tag{A.6}$$

Due to the smoothness properties of B-splines, f is smooth (C^2). Moreover, since the ϕ_i have compact support the “zone of influence” of f_i on f is limited to $[X_{i-2}, X_{i+2}]$. Finally, since $\phi_i \geq 0$ the expansions enables us to construct positive functions by simply imposing that $f_i \geq 0$. It is important to note that the B-spline expansion (A.6) is not an interpolation of f at points (X_i, f_i) : $f(X_i) \neq f_i$.

01 Denote by π the (unique) invariant distribution of M : π verifies

$$02 \int_E \pi(dx) M(x, dy) = \pi(dy)$$

03
04
05 Since the kernel M defined by (36) verifies $M(x, x) > 0$ for any $x \in E$, by Del
06 Moral and Miclo (2003, Proposition 4.4) G^* coincides with the essential infimum
07 of G with respect to π . Let us show that π is absolutely continuous with respect to
08 the Lebesgue measure on E . Consider a subset $U \subset E$ with Lebesgue measure 0.
09 Using the expression of the mutation kernel (36), we have

$$10 \pi(U) = \int_E \pi(dx) M(x, U)$$

$$11 = \int_U \pi(dx) M(x, x) + \int \pi(dx) \int_{y \in U} \frac{\exp[-\frac{1}{2}t(y-x)A^{-1}(y-x)]}{\sqrt{(2\pi)^d |A|}} dy$$

$$12$$

$$13$$

$$14$$

$$15 = \int_U \pi(dx) M(x, x) + 0 \tag{B.2}$$

16
17 since U has measure zero. Therefore using (B.1) we obtain

$$18 \pi(U) \leq \sup_{x \in E} M(x, x) \pi(U) < \pi(U) \tag{B.3}$$

19
20 which entails that $\pi(U) = 0$: π is thus absolutely continuous with respect to
21 the Lebesgue measure. Therefore, the essential infimum of G with respect to π
22 coincides with its global minimum, which gives the result.
23
24

25 REFERENCES

- 26 Achdou, Y., and Pironneau, O. (2002). Volatility calibration by multilevel least squares.
27 *International Journal of Theoretical and Applied Finance* **5**(6), 619–643.
- 28 Ait Sahalia, Y., and Lo, A. (1998). Nonparametric estimation of state-price densities implicit in
29 financial asset prices. *Journal of Finance* **53**, 499–547.
- 30 Andersen, L., and Andreasen, J. (2000). Jump diffusion models: volatility smile fitting and
31 numerical methods for pricing. *Review of Derivatives Research* **4**, 231–262.
- 32 Artzner, P., Delbaen F., Eber, J. M., and Heath, D. (1999). Coherent measures of risk.
33 *Mathematical Finance* **9**(3), 203–228.
- 34 Avellaneda, M., Friedman C., Holmes, and Samperi, D. (1997). Calibrating volatility surfaces
35 via relative entropy minimization. *Applied Mathematical Finance*, March 1997.
- 36 Bäck, T. (1995). *Evolutionary Algorithms in Theory and Practice*. Oxford University Press.
- 37 Brigo, D., and Mercurio, F. (2002). Lognormal mixture dynamics and calibration to market
38 volatility smiles. *International Journal of Theoretical and Applied Finance* **5**(4), 427–446.
- 39 Cerf, R. (1996). The dynamics of mutation-selection algorithms with large population sizes.
40 *Annales de l'Institut Henri Poincaré* **32**(4), 455–508.
- 41 Cerf, R. (1998). Asymptotic convergence of genetic algorithms. *Advances in Applied Probabil-*
42 *ity* **30**(2), 521–550.

- 01 Coleman, T., Li, and Verma, A. (1999). Reconstructing the unknown volatility function. *Journal*
02 *of Computational Finance* **2**(3), 77–102.
- 03 Cont, R. (2006). Model uncertainty and its impact on derivative instruments. *Mathematical*
04 *Finance*, forthcoming.
- 05 Cont, R., and Tankov, P. (2004). Nonparametric calibration of jump-diffusion option pricing
06 models. *Journal of Computational Finance* **7**(3), 1–49.
- 07 Crépey, S. (2003). Calibration of the local volatility in a trinomial tree using Tikhonov
08 regularization. *Inverse Problems* **19**, 91–127.
- 09 Del Moral, P. (2004). *Feynman–Kac Formulae*. Springer, Berlin.
- 11 Del Moral, P., and Miclo, L. (2000). Branching and interacting particle system approximations
12 of Feynman–Kac formulae with applications to nonlinear filtering. *Séminaire de Probabil-*
13 *ités XXXIV (Lecture Notes in Mathematics, Vol. 1729)*. Springer, Berlin, pp. 1–145.
- 14 Del Moral, P., and Miclo, L. (2001). Asymptotic results for genetic algorithms with applications
15 to nonlinear estimation. *Theoretical Aspects of Evolutionary Computing (Nat. Comput. Ser.)*,
16 Kallel *et al* (eds). Springer, Berlin, pp. 439–493.
- 17 Del Moral, P., and Miclo, L. (2003). Annealed Feynman–Kac models. *Communications in*
18 *Mathematical Physics* **235**(2), 191–214.
- 19 Del Moral, P., Kouritzin, M., and Miclo, L. (2001). On a class of discrete-generation interacting
20 particle systems. *Electronic Journal of Probability* **6**(16), 1–26.
- 21 Derman, E., Kani, I., and Chriss, N. (1996). Implied trinomial trees of the volatility smile. *The*
22 *Journal of Derivatives*, Summer 1996.
- 23 Dupire, B. (1994). Pricing with a smile. *RISK* **7**, 18–20.
- 24 Heston, S. (1993). A closed-form solution for options with stochastic volatility with applications
25 to bond and currency options. *Review of Financial Studies* **6**, 327–343.
- 26 Holland, J. H. (1975). *Adaptation in Natural and Artificial Systems*. University of Michigan
27 Press, Ann Arbor.
- 29 Jackson, N., Süli, E., and Howison, S. (1999). Computation of deterministic volatility surfaces.
30 *Journal of Computational Finance* **2**(2), 5–32.
- 31 Jacquier, E., and Jarrow, R. (2000). Bayesian analysis of contingent claim model error. *Journal*
32 *of Econometrics* **94**, 145–180.
- 33 Kallel, L., Naudts, B., and Rogers, A. (eds) (2001). *Theoretical Aspects of Evolutionary*
34 *Computing (Nat. Comput. Ser.)*. Springer, Berlin.
- 35 Ladyzhenskaya, O., Solonnikov, O., and Uralceva, N. (1968). *Linear and Quasilinear Equations*
36 *of Parabolic Type*. (English Translation: American Mathematical Society.)
- 37 Lagnado, R., and Osher, S. (1997). A technique for calibrating derivative security pricing
38 models: numerical solution of an inverse problem. *Journal of Computational Finance* **1**(1).
- 39 Lo, A. (1986). Statistical tests of contingent claims asset-pricing models. *Journal of Financial*
40 *Economics* 143–173.
- 41 Löwe, M. (1996). On the convergence of genetic algorithms. *Expositiones Mathematicae* **14**(4),
42 289–312.
- 43
44
45

01 Madan, D., and Milne, F. (1991). Option pricing with variance gamma martingale components.
02 *Mathematical Finance* **1**, 39–55.

03 Mosegaard, K., and Tarantola, A. (1995). Monte Carlo sampling of solutions to inverse
04 problems. *Journal of Geophysical Research* **100**(B7), 431–447.

05 Nix, A. and Vose, M. D. (1991). Modelling genetic algorithms with Markov chains. *Annals of*
06 *Mathematics and Artificial Intelligence* **5**, 79–88.

07 Samperi, D. (2002). Calibrating a diffusion model with uncertain volatility. *Mathematical*
08 *Finance* **12**, 71–87.

09 Schwefel, H.-P. (1981). *Numerical Optimization of Computer Models*. John Wiley and Sons.

11
12
13
14
15
16
17
18
19
20
21
22
23
24
25
26
27
28
29
30
31
32
33
34
35
36
37
38
39
40
41
42
43
44
45